
Article:
Dhimish, Mahmoud, Holmes, Violeta, Mehrdadi, Bruce et al. (2 more authors) (2018) PV output power enhancement using two mitigation techniques for hot spots and partially shaded solar cells. Electric Power Systems Research. pp. 15-25.

https://doi.org/10.1016/j.epsr.2018.01.002

PV output power enhancement using two mitigation techniques for hot spots and partially shaded solar cells

Mahmoud Dhimish, Violeta Holmes, Bruce Mehrdadi, Mark Dales, Peter Mather
School of Computing and Engineering, University of Huddersfield, United Kingdom

Abstract

Hot spotting is a reliability problem in photovoltaic (PV) panels where a mismatched cell heats up significantly and degrades PV panel output power performance. High PV cell temperature due to hot spotting can damage the cell encapsulate and lead to second breakdown, where both cause permanent damage to the PV panel. Therefore, the design and development of two hot spot mitigation techniques are proposed using a simple, costless and reliable method. The hot spots in the examined PV system was carried out using FLIER i5 thermal imaging camera.

Several experiments have been examined during various environmental conditions, where the PV module I-V curve was evaluated in each observed test to analyze the output power performance before and after the activation of the proposed hot spot mitigation techniques. One PV module affected by hot spot was tested. The output power during high irradiance levels is increased by approximate to 1.25 W after the activation of the first hot spot mitigation technique. However, the second mitigation technique guarantee an increase of the power equals to 3.96 W. Additional test has been examined during partial shading condition. Both proposed techniques ensure a decrease in the shaded PV cell temperature, thus an increase in the output measured power.

Keywords: Hot spot protection; photovoltaic (PV) hot spotting analysis; solar cells; thermal imaging.

1. Introduction

Photovoltaic (PV) hot spots are a well-known phenomenon, described as early as in 1969 [1] and still present in PV modules [2 and 3]. PV hot spots occur when a cell, or group of cells, operates at reverse-bias, dissipating power instead of delivering it and, therefore, operating at abnormally high temperatures. This increase in the cells temperature will gradually degrade the output power generated by the PV module as explained by M. Simon & L. Meyer [4]. Hot spots are relatively frequent in current PV modules and this situation will likely persist as the PV module technology is evolving to thinner wafers, which are prone to developing micro-cracks during the manipulation process such as manufacturing, transportation and installation [5 and 6].

PV hot spots can be easily detected using IR inspection, which has become a common practice in current PV applications as shown in [7]. However, the impact of hot spots on operational efficiency and PV lifetime have been scarcely addressed, which helps to explain why there is lack of widely accepted procedures which deals with hot spots in practice as well as specific criteria referring to acceptance or rejection of affected PV module in commercial frameworks as described by R. Moretón et al [8]. Thus, this paper demonstrates two mitigation techniques which will improve the output power performance of the hot spotted PV modules.

In the past, the increase in the number of bypass diodes (up to one diode for each cell) has been proposed as a possible solution [9 and 10]. However, this approach has not encountered the favor of crystalline PV modules producers since it requires a not negligible technological cost and can be even detrimental in terms of power production when many diodes are activated because of their power consumption as discussed by S. Daliento et al [11].

In addition, the main prevention method for hot spotting is a passive bypass diode that is placed in parallel with a string of PV cells. The use of bypass diodes across PV strings is standard practice that is required is crystalline silicon PV panels [12 and 13]. Their purpose is to prevent hot spot damage that can occur in series-connected PV cells [14]. Bypass diodes turn "on" to provide an alternative current path and attempt to prevent extreme reverse voltage bias on PV strings. The general misconception is that bypassing a string protects cells against hot spotting.

More recently, it has been shown that the distributed MPPT approach suggested by M. Coppola [15] is beneficial for mitigating the hot spot in partially shaded modules with a temperature reduction up to 20 ^{0}C for small shadows. On the other hand, [16 and 17] showing the "inadequateness" of the standard bypass diode, the insertion of a series-connected switch are suited to interrupt the current flow during bypass activation process. However, this solution requires a quite complex electronic board design that needs devised power supply and suitable control logic for activation the hot spot protection device.

A modified bypass circuit for improving the hot spot reliability of solar panels is proposed by S, Daliento [18]. The technique relies on series-connected power MOSFET that subtracts part of the reverse voltage from the shaded solar cell, thereby acting as a voltage divided, while the bypass circuit does not require either a control logic or power supply and can be subtitled to the standard bypass diodes of the PV panels.

This paper presents a simple solution for mitigating the impact of hot spots in PV solar cells. Two techniques are proposed, where both hot spot mitigation techniques consists of multiple MOSTEFs connected to the PV panel which is affected by a hot spot. Several experiments have been examined during various environmental conditions, where the PV module I-V curve was evaluated in each observed test to analyse the output power performance before and after the activation of the proposed techniques.

One PV module affected by a hot spot was tested. After activating the first mitigation technique the output power of the PV module increased by 1.25 W in high irradiance levels, 0.61 W in medium irradiance level and 0.46 W in low irradiance level. Same experiments were carried out using the 2nd proposed hot spot mitigation technique, while the output power increased by 3.96 W in high irradiance levels, 2.72 in medium irradiance levels and 0.98 W in low irradiance levels.

The main contribution of this paper, is the development of a simple, reliable, and fast PV hot spot mitigation technique which reduce the reverse voltage across hot spotted and shaded solar cells, thus mitigating power dissipation and cell temperature. The approach is based on the adoption of a low cost power MOSFETs that sustain part of the reverse voltage, therefore, dissipating a portion of the power in the place of the shaded cells. Differently from [16, 20 and 21], the functioning principle of the proposed approach does not require either power supply or control logic.

This paper is organized as follows: section 2 illustrates the examined PV system, while section 3 describes the proposed hot spot mitigation techniques. Section 4 shows the validation process of the proposed hot spot mitigation techniques using two case studies. Lastly, section 5 demonstrates the conclusion and the future work.

2. Photovoltaic System

2.1 Examined Photovoltaic Module Characteristics

The PV system used in this work comprises a PV plant containing 9 polycrystalline silicon PV modules each with a nominal power of 220 W_p. The SMT6 (60) P solar module manufactured by Romag has been used in this work. The tilt angle of the PV installation is 42^o. The electrical characteristics of the solar module under standard test conditions (STC) are shown in Table 1. In addition, Fig. 1(a) show the overall examined PV plant.

In order to examine the behavior of a PV module, it must be connected to a load. Otherwise, the PV module would not generate an output power, since the PV module will be in open circuit mode. In that case, it is only possible to measure the open circuit voltage and short circuit current. Therefore, in this work, a resistive load was connected to the tested PV module through a maximum power point tracking (MPPT) unit, which can be seen in Fig. 1(b).

The purpose of the MPPT unit is to track the maximum output power of the PV module under various environmental conditions. The MPPT unit is manufactured by Outback Power. This unit has a minimum output efficiency equals to 98.5% [19].

As can be noticed, the PV system does not contain a DC/AC inverter, since this work focuses on the behavior of the PV modules in the DC side. Therefore, MPPT unit with resistive load was used to test the reliability of the proposed methods.

Generally speaking, the performance of the DC/AC inverters used in PV systems are affected by the input power of the PV modules in which it is affected by the PV module's temperature and solar irradiance. Thus, the predictively of the performance for the inverters does not only depends on the input power for the PV modules. Therefore, in this work we will be examining the enhancement of the output power of PV modules under various environmental conditions, and it is intended in the future to examine this improvement using an AC applications.

Table 1 Examined PV electrical characteristics

PV module electrical characteristics	Value
PV peak power	220 W
One PV cell peak power	3.6 W
Voltage at maximum power point (V_{mpp})	28.7 V
Current at maximum power point (I_{mpp})	7.67 A
Open Circuit Voltage (V_{oc})	36.74 V
Short Circuit Current (I_{sc})	8.24 A

I-V curve tracer was also used to plot the I-V curve of the examined PV modules under various experimental conditions. The main specification, including the voltage resolution, and current resolution can be seen in Fig. 1(b). As can be noticed, the error in the measured PV voltage, PV current, solar irradiance and PV module temperature is very limited due to the high accuracy of the I-V tracer, which approximately cost 4,500£.

The AC side of the PV installation has not been considered, since, this work focuses on the behavior of the hot spotted PV modules. As stated in the introduction, there is a rapid decrease in the output power for the hot spotted PV modules. Therefore, this work demonstrates two different techniques to increase the reliability of the hot spotted PV modules, which will be described in section 3.

(a)

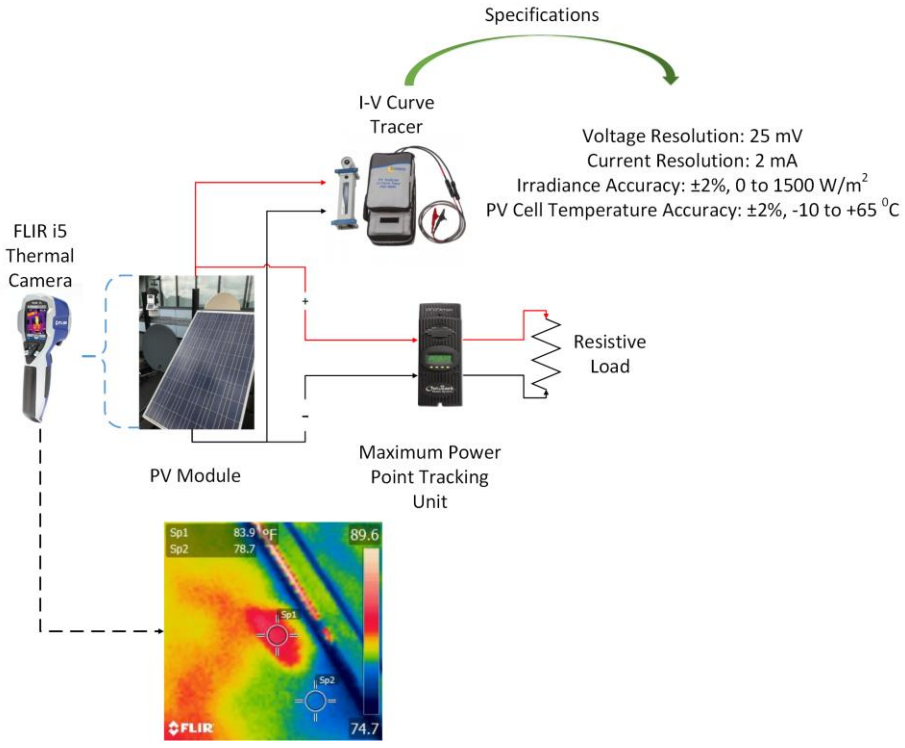

(b)

Fig. 1. (a) Examined PV system installed at the University of Huddersfield, United Kingdom, (b) Structure and the used instruments to examine the hot spotted PV modules

2.2 *Evaluating the Photovoltaic I-V Curve Tracer and i5 FLIR Thermal Camera*

In this section, the output results of the I-V curve tracer shown previously in Fig. 1(b) will be evaluated using various environmental conditions affecting a PV module.

Fig. 2 shows three different I-V curves experimented under high, medium, and low irradiance levels. The theoretical maximum power point (MPP) and measured MPP at each environmental condition is reported, where the accuracy of the I-V curve tracer is equal to:

1. High irradiance level: (185.60 / 186.382) x 100 = 99.58%
2. Medium irradiance level: (107.79 / 108.299) x 100 = 99.53%
3. Low irradiance level: (30.409 / 30.5991) x 100 = 99.38%

As can be seen, the accuracy of the measured MPP and I-V curves is nearly equal to the theoretical data, where the average accuracy in all reported data in Fig. 2 is equal to 99.5%.

The investigation of the hot spots in the examined PV system was carried out using FLIR i5 thermal camera as shown in Fig. 1(b). This camera has a thermal sensitivity equals to 32.18 ^{0}F, where its specification is reported in Table 2.

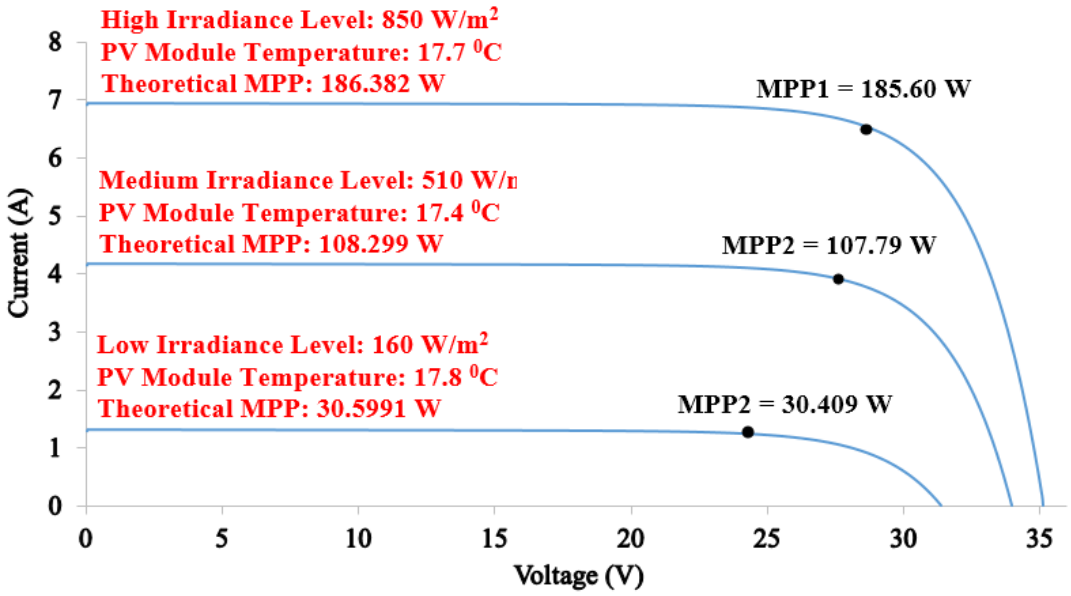

Fig. 2. I-V curve tracer output results for various irradiance levels

Table 2 FLIR i5 camera specification

Comparison	Value
Thermal image quality	100x100 pixels
Field of view	21^0 (H) x 21^0 (V)
Thermal sensitivity	32.18 ^{0}F

Another test was carried out using a PV module affected by one hot spotted solar cell. The thermal image of the examined PV module is shown in Fig. 3(a). As can be seen, the temperature of the hot spotted solar cell is equal to 66.3 F, however, the temperature of the adjacent solar cells are between 60.1 and 57.7 ^{0}F.

The I-V curve of the hot spotted PV module is compared with healthy PV module (PV module without hot spots). The results is shown in Fig. 3(b). The MPP for a PV module without hot spot is equal to 121.61 W. However, the MPP for hot spotted PV module is equal to 115.83 W. Therefore, the power loss due to the hot spot in the examined PV module is equal to 5.78 W.

This experiment was carried out under 621 W/m^2 solar irradiance and the PV modules temperature is approximately equal to 18.2 ^{0}C. Furthermore, according to the measured data in Fig. 2, the average accuracy of the I-V curve tracer is equal to 99.5%. Therefore, the measured data illustrated in Fig. 3(b) has an error in the measurements equals to ±0.5%.

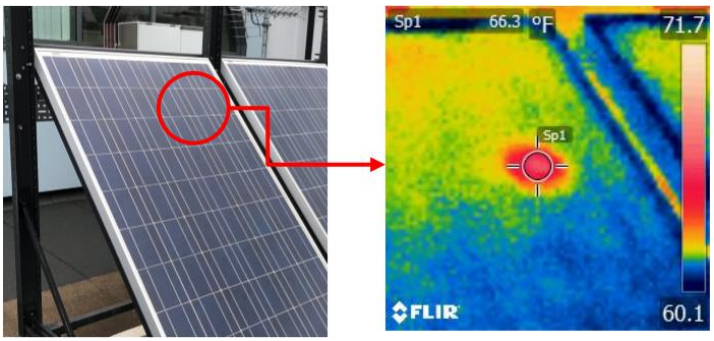

(a)

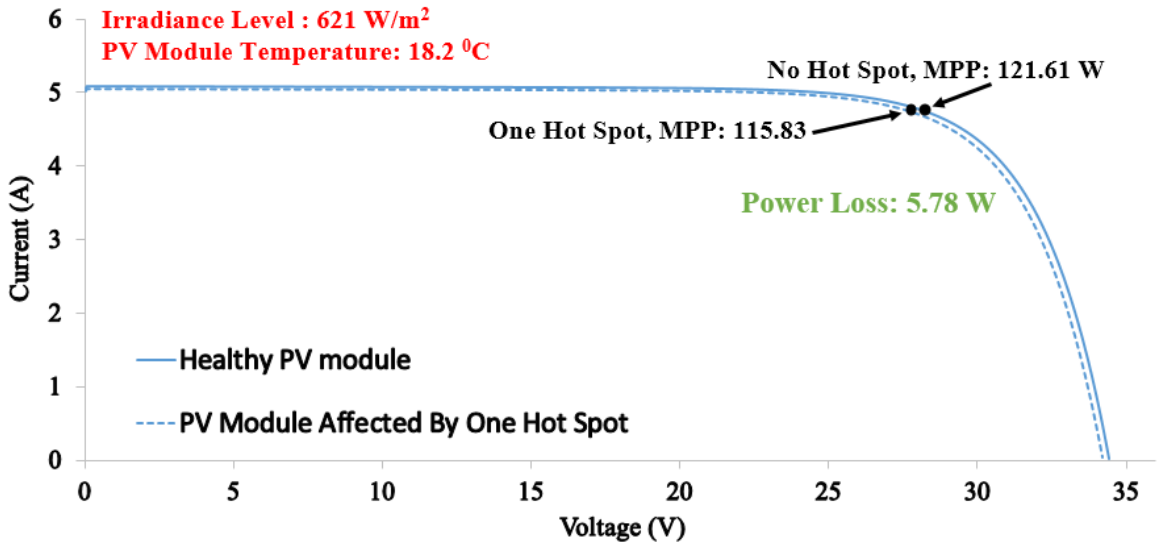

(b)

Fig. 3. (a) Hot Spot detection using FLIR thermal camera, (b) Output results using healthy PV module vs. the hot spotted PV module

3. Proposed Hot Spot Mitigation Techniques

The first proposed hot spot mitigation technique is connected to each PV string in the PV module. As can be seen in Fig. 4(a), the examined PV module used in this work contains three sub strings connected throw bypass diodes.

In order to apply the proposed hot spot protection system, two MOSFETs were connected to each PV string as shown in Fig. 4(b). Switch 1 is in series with the PV string and is normally "on"; it opens when a hot spot condition is detected to prevent further hot spotting. While, switch 2 is in parallel with the PV string and it is normally in "open" mode, it turns "on" to allow a bypass current path when the PV string is open circuited.

Another hot spot mitigation technique was used with the PV module instead of the connection for each MOSFET to the PV strings as shown in Fig. 4(c). The same concept has been applied, where switch 1 is in series with the PV module is normally "on"; it opens when a hot spot condition is detected to prevent further hot spotting. Switch 2 is in parallel with the PV module and is normally "open"; it turn "on" to allow a bypass current path when the PV string is open circuited. The two switch PV protection device has been implemented and connected to the PV panel which contains the hot spot.

As can be noticed, the proposed techniques are simple to implement, where the connection steps is also within the PV module limit, since it requires only to add additional MOSFETs to the hot spotted PV module.

Moreover, Power MOSFETs IRFZ44V were used to implement and test the suggested hot spot mitigation techniques. The MOSFETs drain-to-source breakdown voltage is equal to 60 V, and the voltage drop in drain-to-source as low as 50 mV. Hence, the selection of the MOSFETs plays an important role in the mitigation techniques, therefore, the following MOSFET criteria must be met (any other MOSFET meet these criteria can be used to implement the suggested hot spot mitigation techniques):

1. Low drain-to-source voltage drop: better results in the I-V curve
2. Fast switching speed: to enable fast drop in the temperature of the hot spotted solar cell
3. Low on-resistance: low resistance means more current passes through the PV string
4. High operating temperature
5. Cost effective – for industrial applicability

The cost of the used MOSFETs is equal to 0.85£. Therefore, the total cost for the first and second presented techniques using 3 PV modules are equal to 18£ and 5.1£ respectively.

In the next section, the validation and comparison between both presented hot spot mitigation techniques are illustrated in brief.

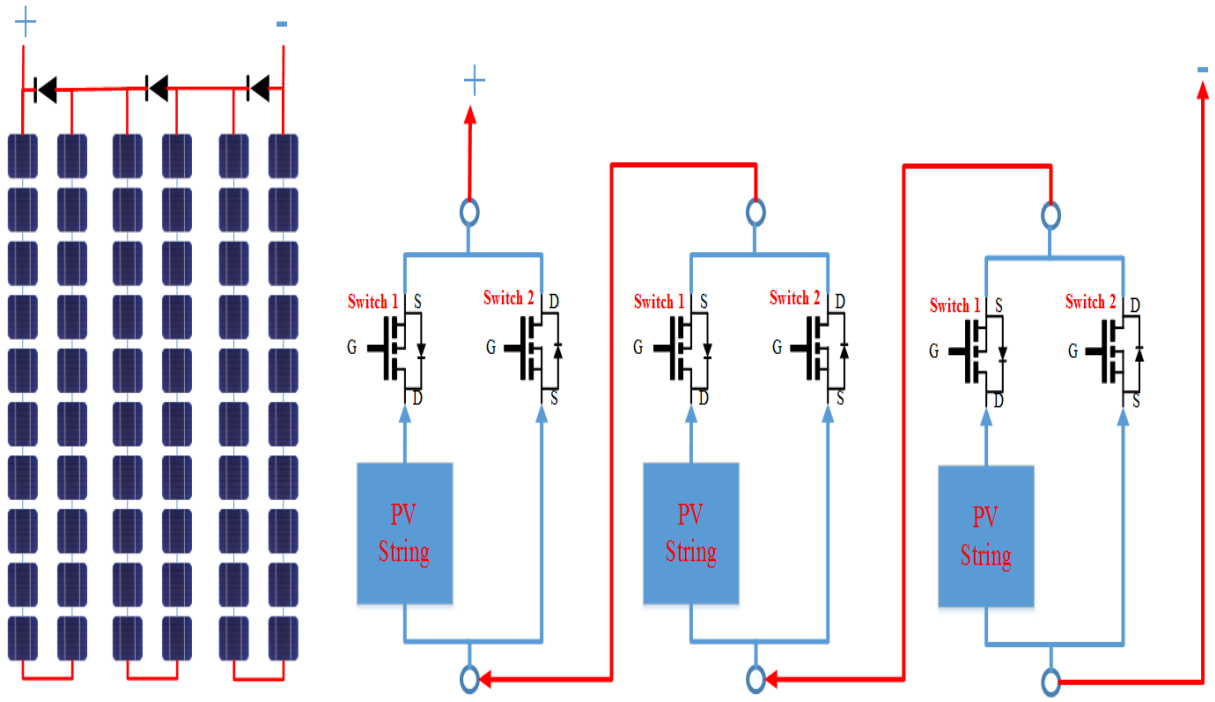

(a) (b)

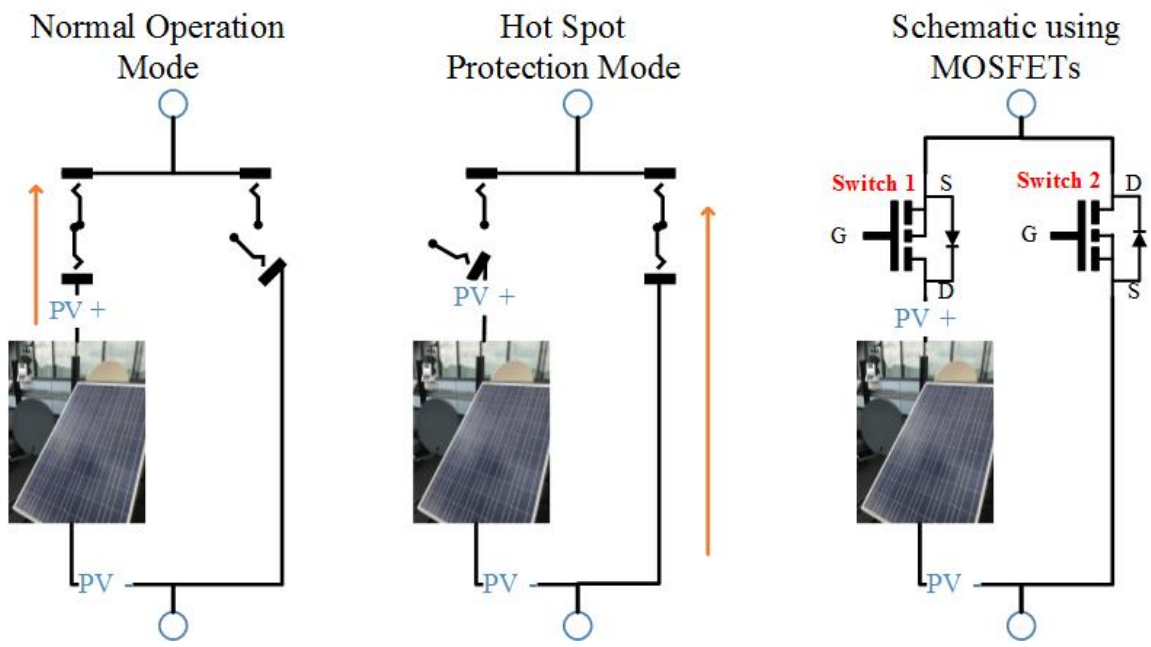

(c)

Fig. 4. (a) The structure of the PV string for the examined PV module, (b) First hot spot mitigation technique, (c) Second proposed hot spot mitigation technique

4. Validation of the Proposed Hot Spot Protection Method

In this section the validation for both proposed hot spot mitigation techniques are demonstrated and compared. The output power has been carried out using the analysis of the I-V curve of the examined PV module, where the detection of the hot spot has been captured using FLIR i5 camera.

4.1 Photovoltaic Hot Spot and I-V Curve Analysis

The proposed hot spotting techniques were tested in an experimental setup with a resistive load powered by the PV module which contains the hot spot, previously shown in Fig. 2, where the MOSFETs are placed in the examined PV module as illustrated in Fig. 4(b) and Fig. 4(c).

There are several stages that have been assessed during the operation of the proposed hot spotting mitigation technique, these stages are describes as follows:

1. **Hot spot mitigation technique 1:**

The results obtained by the first mitigation technique is shown in Fig. 5(a), the results can be described by the following:

A. Before the activation: the temperature of the hot spotted PV solar cell is equal to 70 ^{0}F, while the adjacent (reference) solar cells temperature is equal to 61.5 ^{0}F.
B. 1 minute after the activation: the temperature of the hot spotted PV solar cell reduced to 68.7 ^{0}F, the difference between the hot spotted PV solar cell and the reference solar cell temperature is equal to 7.2 ^{0}F.
C. 2 minutes after the activation: the maximum enhancement of the temperature for the hot spotted PV solar cell is reduced to 67.1 ^{0}F, comparing to 70 ^{0}F before the activation of the mitigation technique.

2. **Hot spot mitigation technique2:**

The results obtained by the first mitigation technique is shown in Fig. 5(b), the results can be described by the following:

A. Before the activation: the temperature of the hot spotted PV solar cell is equal to 70.6 ^{0}F, while the adjacent (reference) solar cells temperature is equal to 61.8 ^{0}F.
B. 1 minute after the activation: the temperature of the hot spotted PV solar cell reduced to 66.3 ^{0}F, the difference between the hot spotted PV solar cell and the reference solar cell temperature is equal to 4.5 ^{0}F.
C. 2 minutes after the activation: the maximum enhancement of the temperature for the hot spotted PV solar cell is reduced to 64.9 ^{0}F, comparing to 70.6 ^{0}F before the activation of the mitigation technique.

As can be noticed, the obtained results for the hot spot mitigation technique 2 has a better performance comparing to technique 1, where the maximum difference between the hot spotted PV solar cell and the adjacent solar cells is equal to 3.1 ^{0}F.

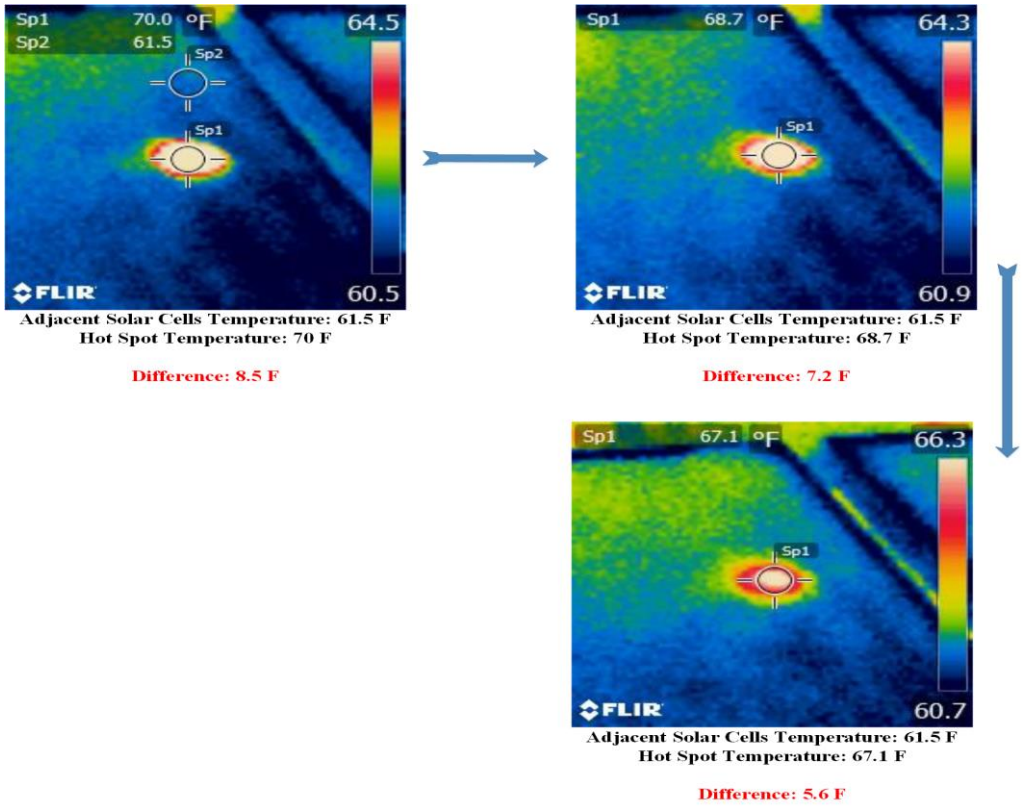

(a)

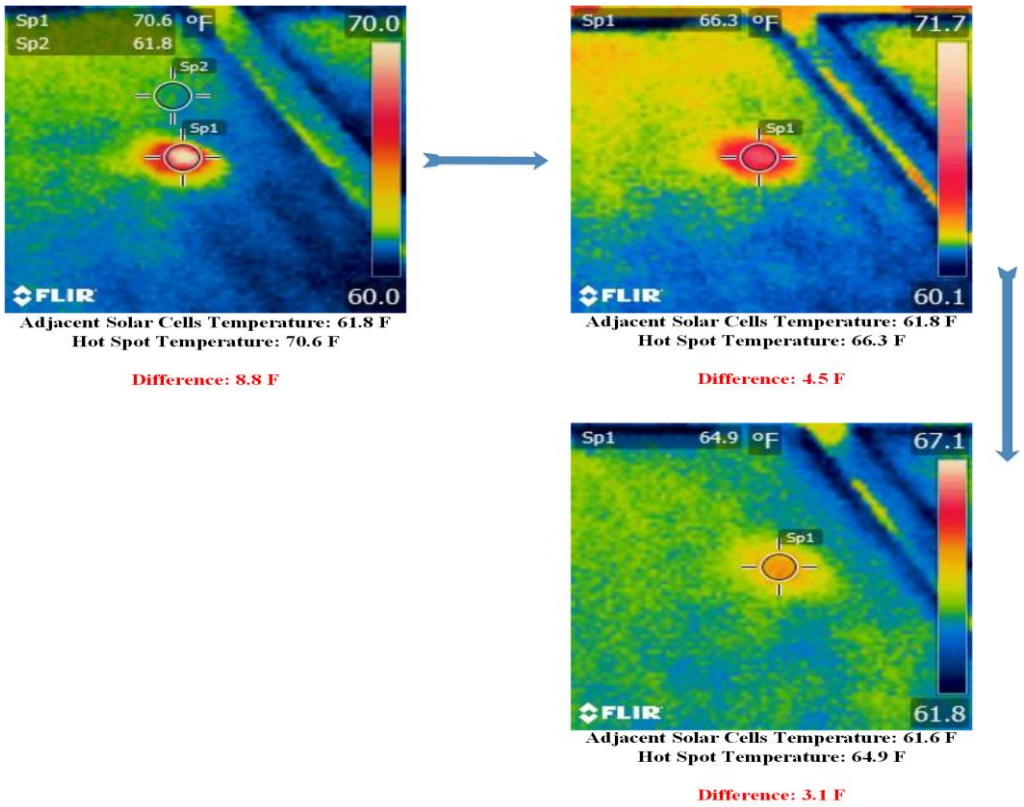

(b)

Fig. 5. (a) Output thermal images the first for hot spot mitigation technique, (b) Output thermal images for the second hot spot mitigation technique

The main reason for the proposed hot spotting mitigation techniques is to improve the output power performance of the examined hot spotted PV module. The value of the power before and after the activation for each proposed technique was monitored in three different irradiance levels: high irradiance level: 840 W/m^2, medium irradiance level: 507 W/m^2 and low irradiance level: 177 W/m^2, while in all tested scenarios, the PV temperature is approximately equal to 16.2 ^{o}C.

Fig. 6(a) shows the output I-V curve of the PV module at high irradiance level. The measured output power after the activation of the proposed 1st technique has a power loss equals to 3.94 W comparing to 5.19 W with no mitigation technique deployed in the PV module. However, the minimum loss in the output power is estimated while activating the 2nd hot spot mitigation technique (P_{loss} = 1.23 W). A brief comparison between both examined techniques are shown in Table 3.

The output I-V curve of the examined PV module under medium and low irradiance levels are shown in Fig. 6(b) and Fig. 6(c) respectively. The output results show a significant improvement in the output power of the 2nd mitigation technique comparing to the 1st technique. Table 3 demonstrates a comparison between the output results in each examined irradiance level.

In conclusion, this section shows the validation and the enhancement of the temperature and the output power generated by the PV module using both proposed hot spot mitigation techniques. Additionally, technique 2 has a better output power performance comparing to the 1st proposed mitigation technique.

Table 3 Comparison between the first and second proposed hot spot mitigation technique using high, medium and low irradiance levels

Irradiance (W/m^2)	Theoretical Power (W)	Case Scenario	Voltage (V)	Current (A)	Power (W)	P_{loss} (W)	Efficiency (%)
High 840	186.4	No mitigation	27.19	6.66	181.18	5.19	97.2
		1st Technique	27.49	6.63	182.44	3.94	97.88
		2nd Technique	28.33	6.53	185.15	1.23	99.33
Medium 507	108.2	No mitigation	26.00	4.02	104.54	3.63	96.64
		1st Technique	26.23	4.00	105.15	3.02	97.20
		2nd Technique	27.21	3.94	107.26	0.91	99.15
Low 177	34.4	No mitigation	23.73	1.39	33.02	1.37	95.99
		1st Technique	24.24	1.38	33.49	0.91	97.33
		2nd Technique	24.94	1.36	34.01	0.39	98.85

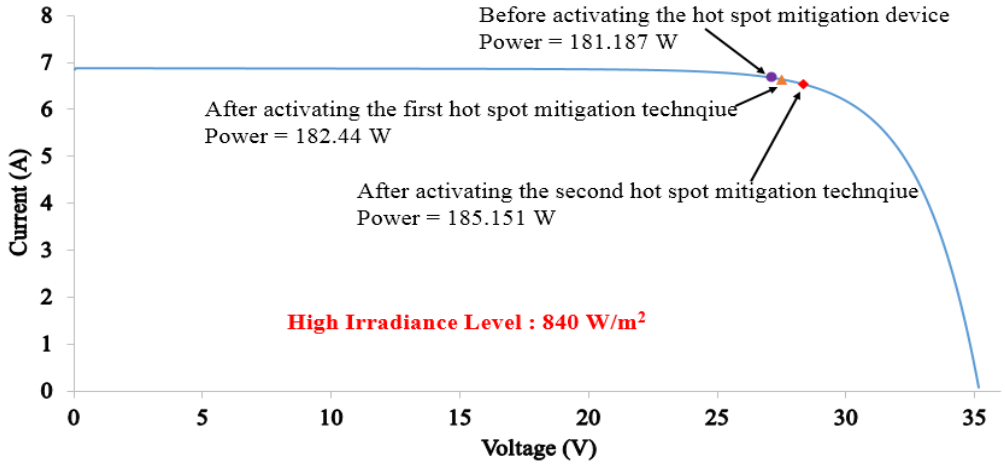

(a)

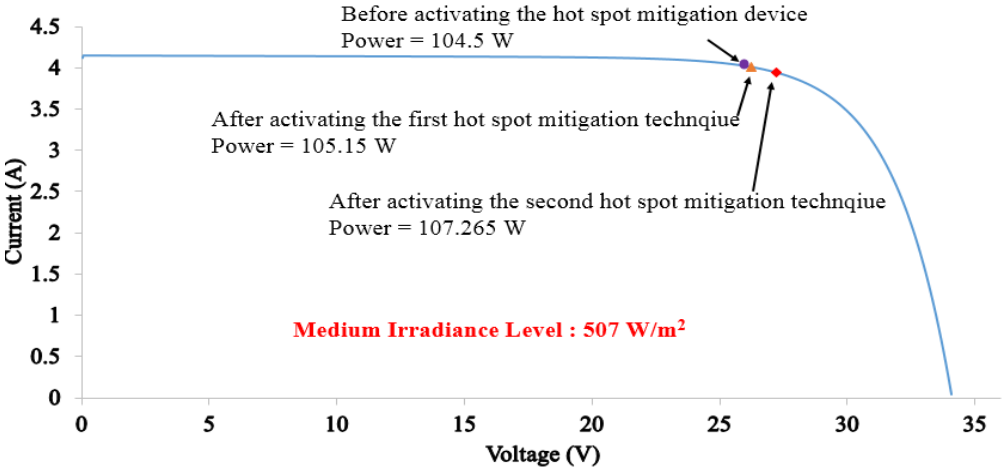

(b)

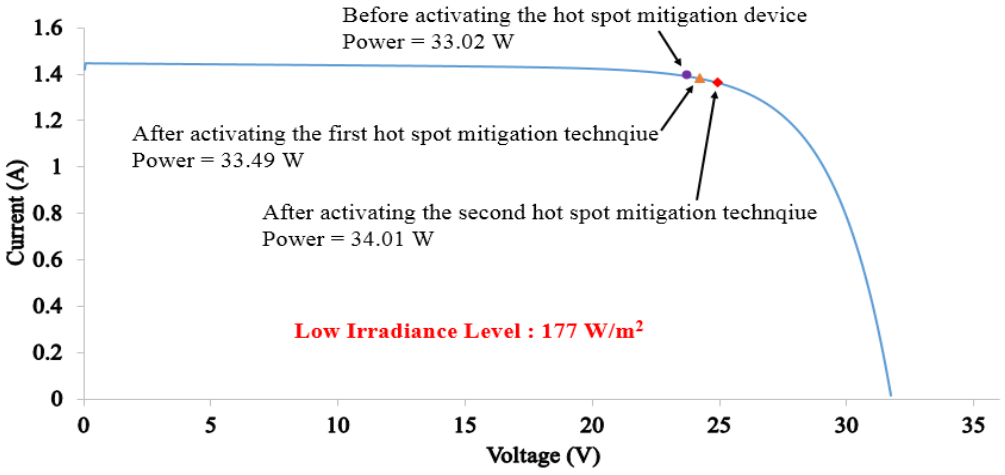

(c)

Fig. 6. Photovoltaic I-V curve. (a) Before and after considering hot spot mitigation techniques at G: 840 W/m^2, (b) Before and after considering hot spot mitigation techniques at G: 507 W/m^2, (c) Before and after considering hot spot mitigation techniques at G: 177 W/m^2

234

4.2 Photovoltaic Partial Shading Analysis

The main purpose of this section is to test the ability of the proposed hot spot mitigation techniques to increase the output power of a PV module during partial shading conditions affecting any PV module. PV Partial shading has been introduced by many researches such as [22 - 25], where there is a limited results which includes the mitigation of the temperature of the shades solar cell.

In order to test the ability of the proposed hot spot mitigation techniques, another experimental test has been carried out on a PV module with partially shaded solar cell. Fig. 7 shows an image of the examined PV module under shaded solar cell using paper opaque object. The PV module was experimented under the same irradiance level which is equal to 784 W/m^2. Moreover, in each tested experiment the temperature of the shaded solar cell was captured using the FLIR i5 camera.

The first test was carried out using the activation of the first proposed hot spot mitigation technique. Fig. 8(a) shows the thermography image of the shaded solar cell before and after the activation of the 1st hot spot mitigation technique. Before the activation, the temperature of the shaded solar cell is equal to 66.6 ^{0}F. The solar cell temperature decreases to a minimum value of 63.9 ^{0}F after the activation of the hot spot mitigation technique. This decrease in the value of the temperature will guarantee an increase in the output power produced by the PV module. As illustrated in Fig. 9(a), the output power before and after the activation is equal to 171.787 W and 172.508 W respectively. Thus, the total increase in the output power is equal to 0.721 W.

The second test was tested using the activating of the second proposed hot spot mitigation technique. Fig. 8(b) displays the thermal images of the examined shaded solar cell before and after activating the mitigation technique. The difference in the temperature of the shaded solar cell is equal to:

(No mitigation) 71.0 ^{0}F – (After activating the 2nd hot spot mitigation technique) 65.3 ^{0}F = 5.7 ^{0}F

In addition, this decrease in the temperature of the shaded solar cell guarantee an increase of the measured maximum power point of the PV module. Fig. 9(b) describes that the total increase in the output measured power is equal to 1.689 W.

In conclusion, this section demonstrates that both proposed hot spot mitigation techniques are useful in case a partial shading conditions have been occurred in the PV module. An enhancement of the temperature and output power of the PV module is guaranteed. Furthermore, the second proposed hot spot mitigation technique shows better performance comparing to the 1st technique.

Fig. 7. Image of the tested PV module under shaded solar cell using paper opaque object

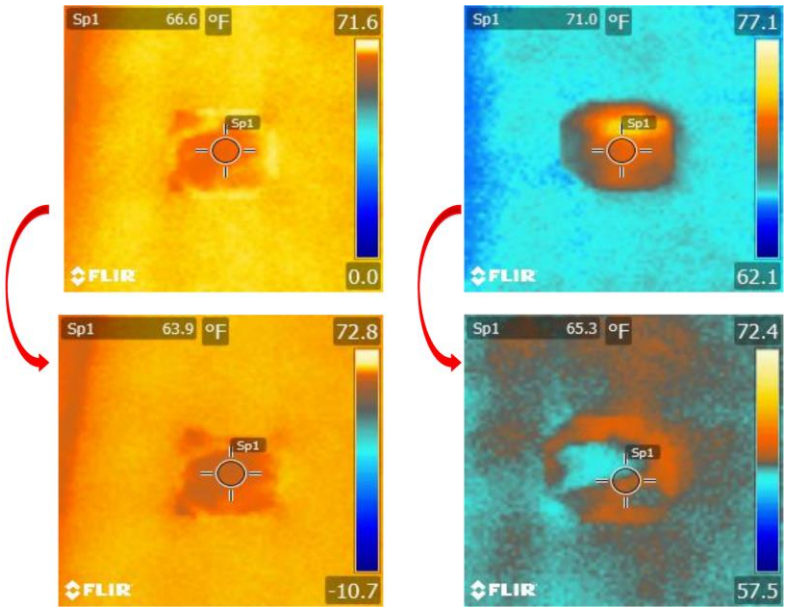

(a) (b)

Fig. 8. (a) Thermographic images of the shaded PV solar cell before and after the activation of the first hot spot mitigation technique, (b) Thermographic images of the shaded PV solar cell before and after the activation of the second hot spot mitigation technique

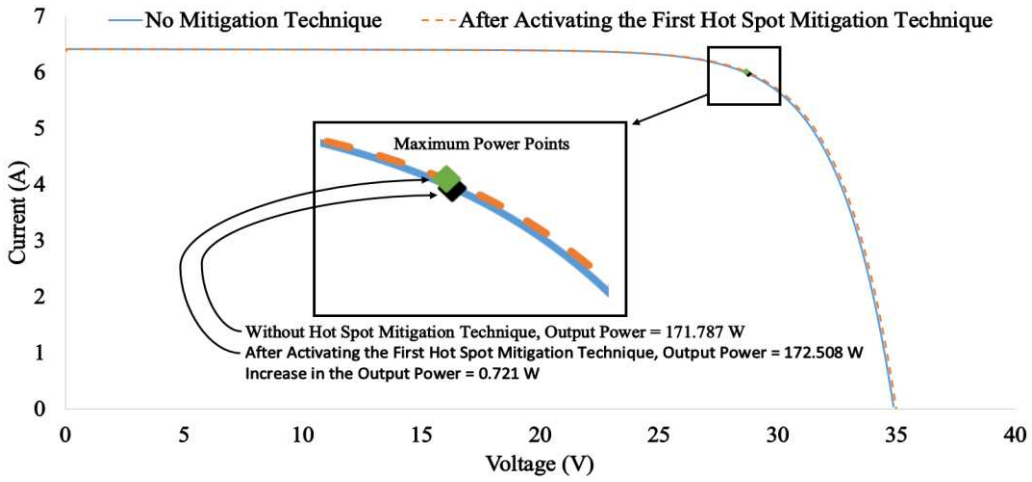

(a)

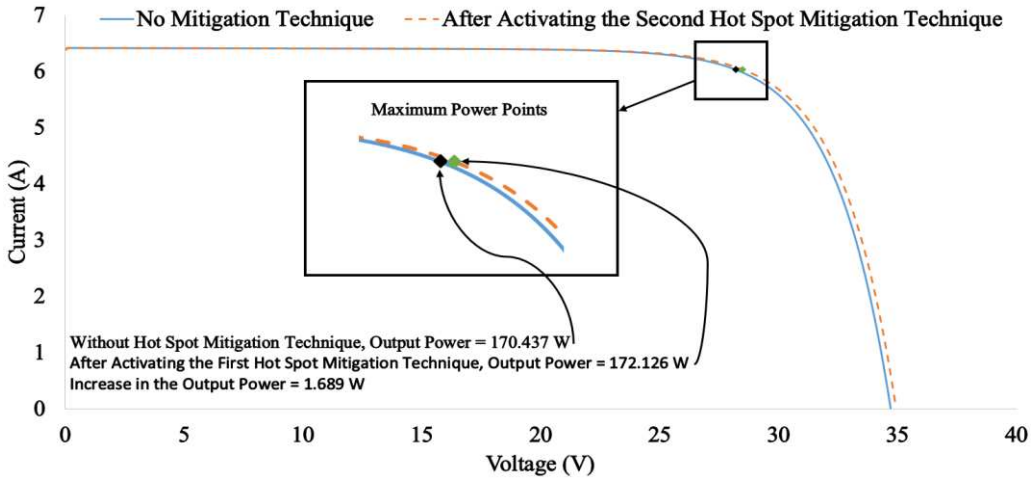

(b)

Fig. 9. Photovoltaic output I-V curve. (a) Before and after activating the first hot spot mitigation technique, (b) before and after activating the second hot spot mitigation technique

5. *Conclusion*

In this paper, the design and development of two hot spot mitigation techniques are proposed. The offered techniques are capable to enhance the output power of PV modules which are effected by hot spots and partial shading conditions. Both techniques use multiple MOSFTEs in the affected PV module, while the detection of hot spots was captured using i5 FLIR thermal imaging camera.

Several experiments have been examined during various environmental conditions, where the PV module I-V curve was evaluated in each observed test to analyze the output power performance before and after the activation of both proposed hot spot mitigation techniques.

One PV module affected by a hot spot was tested. After activating the first mitigation technique the output power of the PV module increased by 1.25 W in high irradiance levels, 0.61 W in medium irradiance level and 0.46 W in low irradiance level. Same experiments have been evaluated using the 2nd proposed hot spot mitigation technique, while the output power increased by 3.96 W in high irradiance level, 2.72 W in medium irradiance level and 0.98 W in low irradiance level.

Additionally, both proposed hot spot mitigation techniques were applied on a shaded PV module. The temperature and output power of the PV module enhanced using both techniques, however, the second mitigation technique shows a better performance comparing to the 1st.

In future, it is intended to improve the hot spot mitigation techniques to work with several PV array configuration systems. In addition, the techniques could be improved to enhance the output power of micro-cracked PV modules.

6. *References*

[1] Blake, F. A., & Hanson, K. L. (1969, August). The hot-spot failure mode for solar arrays. In *Proceedings of the 4th Intersociety Energy Conversion Engineering Conference* (pp. 575-581).

[2] Dhimish, M., Holmes, V., Mehrdadi, B., Dales, M., Chong, B., & Zhang, L. (2017). Seven indicators variations for multiple PV array configurations under partial shading and faulty PV conditions. *Renewable Energy*.

[3] Orduz, R., Solórzano, J., Egido, M. Á., & Román, E. (2013). Analytical study and evaluation results of power optimizers for distributed power conditioning in photovoltaic arrays. *Progress in Photovoltaics: Research and Applications*, *21*(3), 359-373.

[4] Simon, M., & Meyer, E. L. (2010). Detection and analysis of hot-spot formation in solar cells. *Solar Energy Materials and Solar Cells*, *94*(2), 106-113.

[5] Chaturvedi, P., Hoex, B., & Walsh, T. M. (2013). Broken metal fingers in silicon wafer solar cells and PV modules. *Solar Energy Materials and Solar Cells*, *108*, 78-81.

[6] M. Dhimish, V. Holmes, B. Mehrdadi, M. Dales, The Impact of Cracks on Photovoltaic Power Performance, *Journal of Science: Advanced Materials and Devices* (2017), doi: 10.1016/j.jsamd.2017.05.005.

[7] Buerhop, C., Schlegel, D., Niess, M., Vodermayer, C., Weißmann, R., & Brabec, C. J. (2012). Reliability of IR-imaging of PV-plants under operating conditions. *Solar Energy Materials and Solar Cells*, *107*, 154-164.

[8] Moretón, R., Lorenzo, E., & Narvarte, L. (2015). Experimental observations on hot-spots and derived acceptance/rejection criteria. *Solar energy*, *118*, 28-40.

[9] Hasyim, E. S., Wenham, S. R., & Green, M. A. (1986). Shadow tolerance of modules incorporating integral bypass diode solar cells. *Solar cells*, *19*(2), 109-122.

[10] Chen, K., Chen, D., Zhu, Y., & Shen, H. (2012). Study of crystalline silicon solar cells with integrated bypass diodes. *Science China Technological Sciences*, *55*(3), 594-599.

[11] Daliento, S., Mele, L., Bobeico, E., Lancellotti, L., & Morvillo, P. (2007). Analytical modelling and minority current measurements for the determination of the emitter surface recombination velocity in silicon solar cells. *Solar energy materials and solar cells*, *91*(8), 707-713.

[12] Dhimish, M., & Holmes, V. (2016). Fault detection algorithm for grid-connected photovoltaic plants. *Solar Energy*, *137*, 236-245.

[13] Silvestre, S., Boronat, A., & Chouder, A. (2009). Study of bypass diodes configuration on PV modules. *Applied Energy*, *86*(9), 1632-1640.

[14] Dhimish, M., Holmes, V., Mehrdadi, B., & Dales, M. (2017). Diagnostic method for photovoltaic systems based on six layer detection algorithm. *Electric Power Systems Research*, *151*, 26-39.

[15] Coppola, M., Daliento, S., Guerriero, P., Lauria, D., & Napoli, E. (2012, June). On the design and the control of a coupled-inductors boost dc-ac converter for an individual PV panel. In *Power Electronics, Electrical Drives, Automation and Motion (SPEEDAM), 2012 International Symposium on* (pp. 1154-1159). IEEE.

[16] Kim, K. A., & Krein, P. T. (2015). Reexamination of photovoltaic hot spotting to show inadequacy of the bypass diode. *IEEE Journal of Photovoltaics*, *5*(5), 1435-1441.

[17] d'Alessandro, V., Guerriero, P., Daliento, S., & Gargiulo, M. (2011). A straightforward method to extract the shunt resistance of photovoltaic cells from current–voltage characteristics of mounted arrays. *Solid-State Electronics*, *63*(1), 130-136.

[18] Daliento, S., Di Napoli, F., Guerriero, P., & d'Alessandro, V. (2016). A modified bypass circuit for improved hot spot reliability of solar panels subject to partial shading. *Solar Energy*, *134*, 211-218.

[19] M. Dhimish, V. Holmes, M. Dales, Parallel fault detection algorithm for grid-connected photovoltaic plants, Renewable Energy (2017), doi: 10.1016/j.renene.2017.05.084.

[20] Solórzano, J., & Egido, M. A. (2014). Hot-spot mitigation in PV arrays with distributed MPPT (DMPPT). *Solar Energy*, *101*, 131-137.

[21] Dhimish, M., Holmes, V., Mehrdadi, B., Dales, M., & Mather, P. (2017). Photovoltaic fault detection algorithm based on theoretical curves modelling and fuzzy classification system. *Energy*, *140*, 276-290.

[22] Çelik, Ö., & Teke, A. (2017). A Hybrid MPPT method for grid connected photovoltaic systems under rapidly changing atmospheric conditions. *Electric Power Systems Research*, *152*, 194-210.

[23] Khalid, M. S., & Abido, M. A. (2014). A novel and accurate photovoltaic simulator based on seven-parameter model. *Electric Power Systems Research*, *116*, 243-251.

[24] Dhimish, M., Holmes, V., Mehrdadi, B., & Dales, M. (2017). Simultaneous fault detection algorithm for grid-connected photovoltaic plants. *IET Renewable Power Generation*, *11*(12), 1565-1575.

[25] Dhimish, M., Holmes, V., Mehrdadi, B., & Dales, M. (2018). Comparing Mamdani Sugeno fuzzy logic and RBF ANN network for PV fault detection. Renewable Energy, 117, 257-274.